

medium (column 3, lines 48-50), and the applicants agree with all these statements. The applicants further agree with the statement that column 19, line 17 of Albert describes the use of polyisobutylene succinimides such as OLOA 1200 in the suspending fluid of such an electrophoretic medium. However, applicants do not agree that this disclosure of polyisobutylene succinimides such as OLOA 1200 anticipates or renders obvious any of the present claims.

As already noted, present claims 1-23 require that the polymer present in the suspending fluid have a number average molecular weight in excess of about 20,000, and be essentially non-absorbing on the electrophoretic particles. The OLOA 1200 and similar compounds mentioned in Albert do not satisfy either of these requirements. Unfortunately, OLOA 1200, which was a proprietary product formerly marketed by Chevron Corporation, is no longer available, and very little information is publicly available. However, Chevron now markets a replacement product, OLOA 371, which is known to have an average molecular weight of about 1700 (see the marked passage on page 8621 of the enclosed copy of the paper by Kim. J., et al., *Ionic Conduction and Electrode Polarization in a Doped Nonpolar Liquid*, *Langmuir*, **2005**, 8620-8629), an order of magnitude lower than the minimum molecular weight required in present claims 1-23.

Perhaps more importantly, the passage at column 18, line 55 to column 19, line 22 of Albert, which includes the mention of OLOA 1200, specifically identifies all the material there mentioned as charge control agents. As the Examiner is no doubt aware, a charge control agent is a material used in an electrophoretic (or similar) medium to control the charge on the electrophoretic particles. For this purpose, it is essential that the charge control agent be absorbed on to the particles, since manifestly a material which is not absorbed on to a particle cannot control the charge on that particle. In the case of OLOA 1200, such absorption of the additive on to suspended particles is confirmed by the purpose for which the materials were originally developed. As may readily be seen from the manufacturer's website, [www.chevron.com](http://www.chevron.com), the OLOA (Oronite Lubricating Oil

Additive) series of compositions were developed as lubricating oil surfactant additives designed to keep soot and similar small particles stably suspended in lubricating oils. For such a surfactant to be effective, it must obviously absorb or otherwise bind to the particle to be suspended. The OLOA binds to the electrophoretic particles in a similar manner.

It is noted that the Office Action appears to use two separate (and to some extent inconsistent) arguments in asserting that the present claims are unpatentable over Albert. On the one hand (see the penultimate paragraph on page 3) the Office Action asserts that the polyisobutylene succinimide/OLOA 1200 mentioned in Albert has the identical chemical composition to the polyisobutylene mentioned in present claim 8. With respect, applicants have not claimed that all polyisobutylenes and derivatives thereof can be used in the present invention; since claim 8 depends (ultimately) from claim 1, claim 8 is inherently restricted to polyisobutylenes having a molecular weight of at least 20,000 and being non-absorbing on the electrophoretic particles. For the reasons mentioned above, the polyisobutylene succinimide mentioned in Albert is not such a polymer and does not inherently meet the requirements of the present invention.

On the other hand (see the first two paragraphs on page 4), the Office Action asserts that it would be obvious to a person skilled in the art to vary the molecular weight and absorptive properties of the polyisobutylene succinimide disclosed in Albert to produce an electrophoretic medium of the present invention. While some variation in molecular weight would no doubt be within the level of skill in the art, the Examiner has not suggested why a skilled person would vary molecular weight by an order of magnitude, especially since it does not appear that polyisobutylene succinimides are made with the molecular weight range required by present claim 1. More importantly, in view of the explicit teaching of Albert that the polyisobutylene succinimide is intended to function as a charge control agent, it would not be obvious to the skilled worker to modify this material so that it would not absorb on the electrophoretic particles, since the skilled worker would know that such absorption on to the particles is essential if the

material is to function as a charge control agent; it is settled law that it is not obvious to modify a device or system in a manner which destroys the intended function of the device or system.

The foregoing remarks are applicable to all of claims 1 to 23. Claims 24-27 all specify a minimum molecular weight of 200,000 for the polyisobutylene. For the reasons given above relating to the molecular weight limit of 20,000 for claims 1-23, Albert does not disclose a polymer having anything near the molecular weight required by claims 23-27, nor would it be obvious to one of ordinary skill in the art to modify the molecular weight of the polymer by about two orders of magnitude to produce a medium in accordance with any of claims 24-27.

Claim 28 specifies (*inter alia*) that the suspending fluid contain a polymer "substantially free from ionic or ionizable groups". The polyisobutylene succinimide used in Albert is of course not substantially free from ionic or ionizable groups but rather is heavily loaded with such groups, namely quaternizable imide and amide groups. (Despite the "succinimide" nomenclature used, in practice a substantial fraction of the material is hydrolyzed with the succinimide ring opening to produce amide and hydroxyl groups in place of the original imine grouping; however, the distinctions discussed below apply regardless of the extent of this hydrolysis.) Hence, Albert does not describe an electrophoretic medium in accordance with claim 27. Furthermore, since the ability of the polyisobutylene succinimide to act as a charge control agent depends upon the presence of the substantial numbers of ionizable groups, a skilled worker would not modify the polymer to eliminate such groups since this modification would destroy the function of the material as a charge control agent.

For the foregoing reasons, the 35 USC 103(a) rejection is unjustified and should be withdrawn.

Reconsideration and allowance of all claims in this application is respectfully requested.

*Webber*  
*Serial No. 10/063,236*  
*Response to Office Action dated August 2, 2005*  
*Page 5*

Since the normal period for responding to the Office Action expired November 2, a Petition for a one-month extension of this period is filed herewith.

Respectfully submitted



David J. Cole  
Registration No. 29629

E INK Corporation  
733 Concord Avenue  
Cambridge MA 02138-1002

Telephone (617) 499-6069  
Fax (617) 499-6200  
E-mail dcole@eink.com

# Ionic Conduction and Electrode Polarization in a Doped Nonpolar Liquid

Junhyung Kim,<sup>†,‡</sup> John L. Anderson,<sup>\*,†,§</sup> Stephen Garoff,<sup>†,||</sup> and  
Luc J. M. Schlangen<sup>⊥</sup>

Department of Chemical Engineering, Carnegie Mellon University, Pittsburgh, Pennsylvania 15213, Center for Complex Fluids Engineering, Carnegie Mellon University, Pittsburgh, Pennsylvania 15213, Department of Chemical Engineering, Case Western Reserve University, Cleveland, Ohio 44106, Department of Physics, Carnegie Mellon University, Pittsburgh, Pennsylvania 15213, and Philips Research Laboratories, Photonic Materials and Devices, Eindhoven, The Netherlands

Received September 10, 2004. In Final Form: June 8, 2005

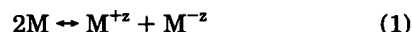
Electrical current versus potential relationships were measured for solutions of dodecane containing the charge control agent poly(isobutylene succinimide) (PIBS) at various concentrations. Both one-dimensional (parallel planar electrodes) and two-dimensional (strip electrodes) fields were studied. The initial current was proportional to the applied voltage for both electrode configurations. Using the initial decay rate of the current ( $t < 0.5$  s) in the planar electrode cell and the Gouy–Chapman model for electrode polarization, we determined the diffusion coefficient of the charge carriers (micelles) in the solution, from which we calculated their effective radius to be 10 nm. The constancy of the carrier radius over a 7-fold change in PIBS concentration, along with the proportionality between conductivity and concentration, supports the hypothesis that the charged species result from the interactions between two micelles. The experimentally determined geometric factor (cell constant) relating current to applied potential at time zero for the strip electrode cell agrees with the value predicted from the solution of Laplace's equation for the electrical potential in this system. The intermediate-time (0.5–3.0 s) decay rate of current was faster than predicted from the classical Gouy–Chapman theory of the double layer, possibly because of volume fraction effects in the double layer. The very long-time (minutes to hours) residual current that we observed is not explained, but we suspect that some charge transfer across the electrode must have occurred because there was insufficient ion capacity (i.e., amount of PIBS) in the solution to account for the total charge transferred through the cell.

## Introduction

One approach to producing optical displays that have paperlike reflective properties involves the movement of pigments using electric fields. An example is the concept of electrophoretic ink, in which particles are either rotated<sup>1</sup> or translated<sup>2,3,4,5,6,7</sup> within a pixel-size compartment using an electric field. In these situations, a field of order  $10^5$  V/m or greater must be sustained for a second in the liquid in which the particles are suspended. To achieve this level and duration of the field, the liquid must have a low conductivity;<sup>8,9</sup> however, the conductivity must be suf-

ficiently high that the particles have some charge and will move by an electrophoretic mechanism. Furthermore, the liquid should not allow electrode reactions that could alter its chemical composition over hundreds of cycles. This means water and lower alcohols are not useful in this application.

In pure nonpolar liquids, such as aliphatic hydrocarbons, free charges are almost nonexistent. Adding a "charge control agent" (CCA) stabilizes free charges in the liquid and on the surfaces of particles.<sup>10,11</sup> The addition of these agents also provides a stable conductivity. The conductivity of such aliphatic hydrocarbon/CCA mixtures is sometimes proportional to the concentration of the CCA, which is consistent with a model that envisions micelles of the CCA exchanging charge with each other.<sup>10,12,13</sup>



Even assuming this mass action principle is the source of charge carriers, the model is simplified in that each exchange is assumed to result in a valence of  $z$  charges

\* To whom correspondence should be addressed. Office of the Provost, Case Western Reserve University, 10900 Euclid Avenue, Cleveland, OH 44106-7001. Phone: 216-368-4346. Fax: 216-368-4325. E-mail: johna@case.edu.

<sup>†</sup> Department of Chemical Engineering, Carnegie Mellon University.

<sup>‡</sup> Center for Complex Fluids Engineering, Carnegie Mellon University.

<sup>§</sup> Case Western Reserve University.

<sup>||</sup> Department of Physics, Carnegie Mellon University.

<sup>⊥</sup> Philips Research Laboratories.

(1) Gyricon Media, <http://www.gyriconmedia.com>.

(2) Comiskey, B.; Albert, J. D.; Yoshizawa, H.; Jacobson, J. *Nature* **1998**, *394*, 253.

(3) Murau, P.; Singer, B. *J. Appl. Phys.* **1978**, *49*, 4820.

(4) Dalisa, A. L. *IEEE Trans. Electron Devices* **1977**, *ED-24* (7), 827.

(5) Elliot, G. *Radio Electron. Eng.* **1976**, *46*, 281.

(6) Hopper, M. A.; Novotny, V. *IEEE Trans. Electron Devices* **1979**, *ED-26* (8), 1148.

(7) Liang, R. C., <http://www.sipix.com>.

(8) Croucher, M. D.; Harbour, J.; Hopper, M.; Hair, M. L. *J. Photogr. Sci. Eng.* **1981**, *25*, 80.

(9) Croucher, M. D.; Drappel, S.; Duff, J.; Lok, K.; Wong, R. W. *Colloids Surf.* **1984**, *11*, 303.

(10) Morrison, I. D. *Dispersion and Aggregation: Fundamentals and Applications*; Proceedings of the Engineering Foundation Conference, Palm Coast, Florida, 1992.

(11) Kornbrekke, R. E.; Morrison, I. D.; Oja, T. *Langmuir* **1992**, *8*, 1211.

(12) Dukhin, A. S.; Goetz, P. J. "How nonionic 'electrically neutral' surfactants enhance electrical conductivity and ion stability in nonpolar liquids", submitted for publication, 2004.

(13) Dukhin, A. S.; Goetz, P. J. *Ionic Properties of Non-Polar Liquids and Dispersions with Non-Ionic Surfactants and Means of Their Characterization*; Presentation at the International Electrokinetics Conference, Pittsburgh, PA, 2004.

per charge carrier rather than allowing for a distribution of values of  $z$ . Here we assume  $z = 1$ .

Direct experimental evidence exists for the formation of micelles.<sup>14,15</sup> Presumably, the core of the micelle is sufficiently polar to stabilize free charges or contains water molecules that aid in the stabilization of the ions. During a binary collision, one micelle picks up an unbalanced ion (e.g.,  $H^+$ ) and the other micelle thus experiences a deficit charge. Impurities might also play a role in this ionization. In this model, the charge carriers have valences of  $\pm z$  and the mobility of each carrier is that of the micelles, which are assumed to be uniform in size. The conductivity of the solution in this model is given by the expression used with simple electrolytes in a polar liquid such as water:<sup>16</sup>

$$K = \frac{2z^2 F^2 DC}{R_g T} \quad (2)$$

where  $F$  is Faraday's constant,  $R_g T$  is the thermal energy per mole,  $D$  is the diffusion coefficient of each charge carrier, and  $C$  is the concentration of pairs of the charge carriers. The solution is assumed to be electroneutral. A direct measurement of  $K$  gives the product  $z^2 DC$ . Note that in systems such as the one studied here  $C$  is a small fraction of the total concentration of the CCA.

The description of conductive processes within nonpolar liquids containing a CCA is far from complete.<sup>17–21</sup> This is especially true for the electrophoretic migration of particles and polarization processes at electrodes, though the work of Morrison and Tarnawsky<sup>22</sup> established a consistent picture for conduction and particle electrophoresis in dodecane with poly(isobutylene succinimide) (PIBS) as the CCA. Separating electrode processes from conductive processes is not generally possible except at high frequencies and in one-dimensional fields. Even in the absence of electrode chemistry, the double layer at the electrode surfaces plays a role in determining the time evolution of the current at fixed applied potential. Two-dimensional systems with polarized electrodes are even more complex because of the nonuniform current, and hence uneven polarization along the surface of the electrodes.

In this paper, we report the results of experiments with dodecane containing PIBS as the charge control agent. By using planar and strip electrodes, we studied both one- and two-dimensional fields. Data for initial currents (before electrode polarization is significant) are used to establish the linearity of the system in both electrode configurations. We use the time constant describing the initial decay rate of the current in the planar electrode cell, with a model for the double layer on the electrodes, to determine the diffusion coefficient and concentration of the charge carriers. Using the independent measurements of the conductivity of the solutions, we determine the effective cell constant for the strip electrode cell from the initial current/potential relationship and compare it with theoretical predictions based on numerical solution

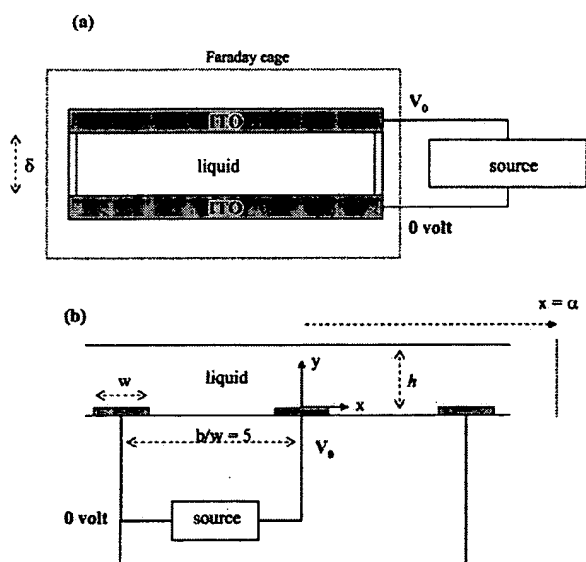


**Figure 1.** Electrode configurations. The active electrode surfaces (strips) in both cases were  $0.11 \mu\text{m}$  thick films of ITO on glass (note that the thickness of the strips is exaggerated in the figure). (a) planar electrode cell (area =  $7.3 \text{ cm}^2$ ,  $\delta = 190 \mu\text{m}$ ) (b) strip electrode cell ( $w = 30 \mu\text{m}$ ,  $b = 150 \mu\text{m}$ ,  $h = 30$  or  $120 \mu\text{m}$ ).  $\alpha$  is an imaginary boundary defined by eq 10.

of Laplace's equation for the electrical potential. Finally, we report observations of a long-time (minutes to hours) residual current and speculate on its possible cause.

## Experiments

Solutions were made by mixing dodecane (99+%, Aldrich Co) and OLOA 371 (Chevron Oronite Co). Neither the dodecane nor the mixtures were dried, and no special measures were taken to control the humidity. OLOA 371<sup>23</sup> is very similar to the material known as OLOA 1200<sup>24</sup> in the literature. Both are primarily poly(isobutylene succinimide) (PIBS) having a molecular architecture with three parts: a section with multiple amine groups, a polyisobutylene tail designed for steric stabilization, and a succinimide moiety linking the other two parts. For our system (OLOA 371) we use an average molecular weight of 1700, and we interchange the names OLOA and PIBS equivalently.

The conductivity ( $K$ ) of the solutions was measured with a Scientifica 627 meter and probe (Scientifica, Princeton, NJ). The measurements for a given solution were constant over times of 1 h but the value of  $K$  increased slightly over longer periods. Carbon black (Black Pearl 130, Cabot Corp), which was processed in a blender to a size of about  $1 \mu\text{m}$ , was added in small amounts to some of the solutions in order to study electrophoretic migration of the particle in two-dimensional electric fields.<sup>24</sup> Although the carbon black increased the solution conductivity, its presence did not change the  $dc$  current characteristics in any fundamental way.

Current–potential relations were determined with the electrode configurations shown in Figure 1. The electrodes were  $0.11 \mu\text{m}$  films of tin-doped indium oxide (ITO) on glass prepared at Philips Research Laboratories (Eindhoven, The Netherlands). With the planar electrodes, the potential of the upper electrode was  $V_0$  volts and the lower electrode was held at ground potential (see Figure 1a). In the case of the strip electrodes, the outer two strips were held at ground potential, and the middle strip was clamped at potential  $V_0$  (see Figure 1b). With the planar electrodes, the contact between electrode and circuit was made

(14) Morrison, I. D. *Colloids Surf. A: Physicochem. Eng. Aspects* 1993, 71, 1.

(15) Kornbrenke, R.; personal communication.

(16) Newman, J. S. *Electrochemical Systems*; Prentice Hall: Englewood Cliffs, NJ, 1991.

(17) Douwes, C.; Waarden, M. V. *J. Inst. Pet.* 1967, 53, 237.

(18) Novotny, V.; Hopper, M. A. *J. Electrochem. Soc.: Solid-State Sci. Technol.* 1979, 126, 2211.

(19) Denat, A.; Gosse, B.; Gosse, J. P. *J. Electrostatics* 1982, 12, 197.

(20) Walmsley, H. L. *Inst. Phys. Conf. Ser., session II* 1983, 66, 45.

(21) Gosse, J. P. *NATO Adv. Study Inst. Ser. B, Phys.* 1988; 193, 503.

(22) Morrison, I. D.; Tarnawsky, C. J. *Langmuir* 1991, 7, 2358.

(23) Desenne, G.; Chevron Oronite S. A. France, GDES@chevrontexaco.com, <http://www.aronite.com> 2004.

(24) Kim, J.; Anderson, J. L.; Garoff, S.; Schlangen, L. J. M. Movement of Colloidal Particles in Two-Dimensional Electric Fields. Submitted for publication, 2005.

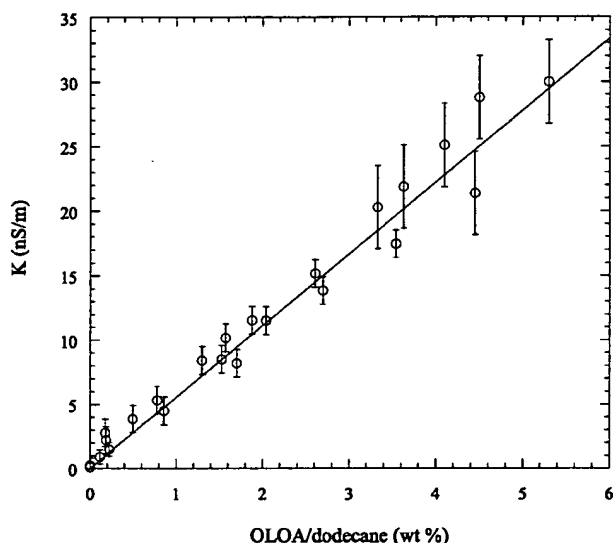


**Figure 2.** Conductivity as a function of OLOA concentration.  $K$  was measured with the conductivity probe. The error bars are based on the standard deviation of the measured conductivities. The line is given by eq 3.

by miniature alligator clips, while the contact with the strips was achieved by a flexible film circuit attached to a pin-connector. In both electrode configurations the potential difference was established at time zero and held constant using a Keithley 2400 Sourcemeter. The current was measured as a function of time at intervals of 57 ms with a Keithley 6514 electrometer connected to a personal computer using LabView 6.1 (National Instrument) for data analysis.

### Results and Discussion

The results for the conductivity of the OLOA/dodecane solutions are shown in Figure 2; these data do not include the results for the solutions containing carbon black. The following equation is a least-squares fit to the data:

$$K = (5.72 \pm 0.14)C_{OL} \quad (3)$$

where  $K$  is in nS/m and  $C_{OL}$  is wt %. These results are in good agreement with data published by Morrison.<sup>10</sup> Although the data show  $K$  is proportional to  $C_{OL}$ , the origin of the standard deviation among the measurements is not known. The temperature variation of  $\pm 2$  °C (about a mean of 24 °C) would yield only a 4% uncertainty due to variations in the viscosity of the liquid.

An example of current versus time for the planar cell is shown in Figure 3. The current decayed in about 10 s to a nearly constant value which we call the "residual current" ( $I_{res}$ ). The values of residual current presented later were measured 10 s after the voltage clamp was applied, but they persisted for up to hours at a lower but comparable level.

After first discussing a general model for ion transport in the solution, we report initial currents ( $I_0$ ) when the voltage ( $V_0$ ) was first applied. The short-time current transients for the planar cells are then analyzed to obtain the concentration and the diffusion coefficient, and hence size, of the charge-carrying elements of the solutions. Finally, we address the intermediate and long time currents in the system.

**Model for Ion Transport.** The basic model for the flux ( $N_i$ ) of charge carrying species of valence  $z_i$ , and

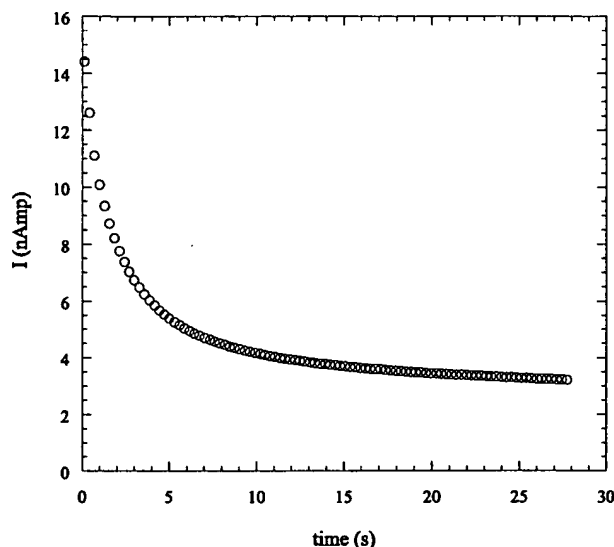


**Figure 3.** Example of current versus time in the planar electrode cell with 0.5 wt % OLOA.  $V_0 = 1.0$  V. Measurement errors were smaller than the symbols.

concentration  $C_i$  is given by the Nernst Planck equation. In the absence of fluid convection, this relation is

$$N_i = -D_i \left[ \nabla C_i + \frac{z_i F}{R_g T} C_i \nabla \Phi \right] \quad (4)$$

where  $\Phi$  is the electrical potential and  $D_i$  is the diffusion coefficient of the charge carrier. Conservation of the charge carriers requires

$$\frac{\partial C_i}{\partial t} = -\nabla \cdot N_i + r_i \quad (5)$$

where  $r_i$  is the rate of production of species  $i$  per unit volume of liquid. With strong electrolytes in water, nearly all of the electrolyte is ionized so  $r_i = 0$ . However, if charged micelles are formed as indicated in eq 1, then this term might be important because it would restore charge carriers as they are depleted due to migration in the electric field. Finally, the ions interact through the mean electrical potential ( $\Phi$ ) which is related to the free charge by Poisson's equation

$$\nabla^2 \Phi = -\frac{F}{\epsilon} \sum_i z_i C_i \quad (6)$$

where  $\epsilon$  is the dielectric permittivity of the liquid. The above nonlinear relations define both the concentration of the ions and the electrical potential, given the boundary and initial conditions on the concentrations and electrical potential. Verschueren et al.<sup>25</sup> numerically solved these equations in a modified form for a planar electrode configuration to derive the valence, concentration and size of the charge carrying species in OLOA/dodecane solutions. They neglected the formation or recombination of charge carriers ( $r_i = 0$ ).

Here we take a simpler but approximate approach to analyze the initial currents and short-time current transients to obtain the concentration of charge carriers and their size. At time zero, when the potential difference

(25) Verschueren, A. R. M.; van Zandwijk, G. C.; Notten, P. H. L., Strubbe, F.; Neyts, K.; Schlangen, L. J. M. submitted for publication, 2005.

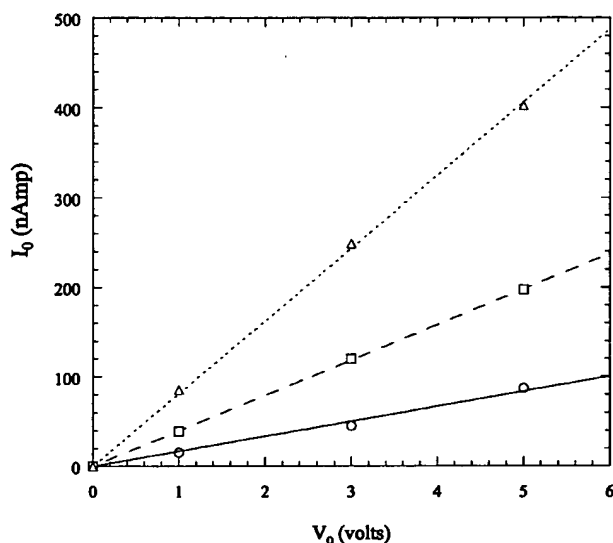


**Figure 4.** Initial current versus applied potential in the planar electrode cell. Circle: 0.50% OLOA; square: 1.57% OLOA; triangle: 3.63% OLOA. The line is a best fit of the data. Measurement errors were smaller than the symbols.

across the electrodes is first applied, the concentration of charge carriers is uniform in the solution and  $C_+ = C_- = C$ . The time dependent term in (5) is zero in the bulk of the solution, but it is nonzero near the electrodes as charge carriers migrate to or from their surfaces, thus created space charge. At early times, the following equation holds in the liquid at distances much greater than the Debye length ( $\kappa^{-1}$ ) of the solution

$$\nabla^2 \Phi = 0 \quad (7)$$

This relation is invalid within distances of order  $\kappa^{-1}$  from the electrode surface, the region of space charge which builds because charge is not exchanged between the electrode and the solution. Our approach is to solve the above equation at time zero, when the space charge in the double layers at the electrode surfaces is insignificant. Within the double layer of charge, Poisson's equation must be used to relate the potential drop across the double layer to the build-up of charge carriers at the surface of the electrode. This is done later using the classical Gouy-Chapman theory for the double layer. This approach of splitting the liquid into two regions, the bulk solution where eq 7 holds and the polarized double layers at the electrode surfaces where eqs 5 (with  $r_i = 0$ ) and 6 must be used, is valid under two conditions. First, the bulk solution must not be depleted of charge carriers so that the conductivity remains constant; and second, the thickness of the polarized layer must be small compared to the distance between the electrodes. At the critical experimental times noted below ( $t = 0, 0.5$ , and  $3.0$  s) these two conditions should be met, as discussed later.

**Initial Current vs Applied Potential.** The initial currents ( $I_0$ ) are proportional to the applied potential for both electrode configurations, as shown in Figures 4 and 5. The proportional relationship means that the initial currents represent purely conductive processes in the solution, without measurable effects of polarization or charge-transfer reactions at the electrodes. The ratio of the solution conductivity ( $K$ ) to the geometric cell constant

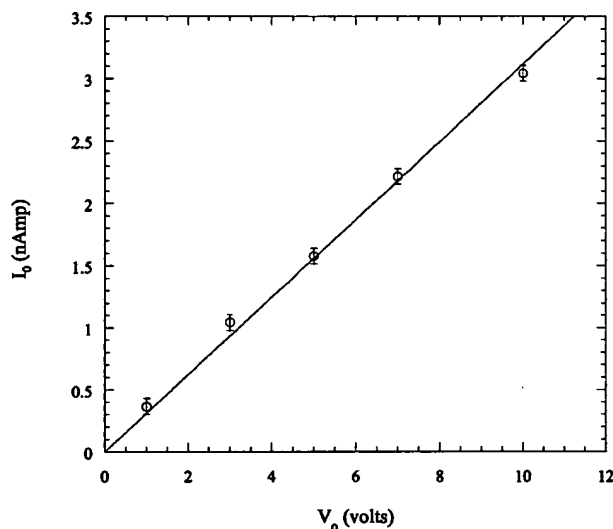


**Figure 5.** Initial current versus applied potential in the strip electrode cell ( $C_{OL} = 3.43$  wt %,  $h = 120$   $\mu$ m). The line is a best fit of the data.

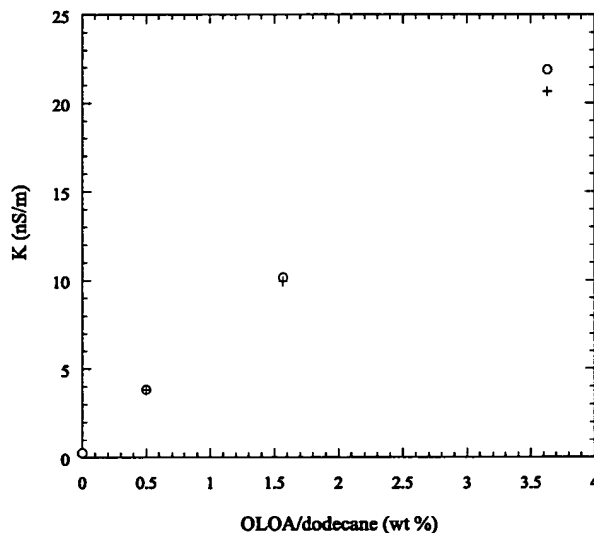


**Figure 6.** Comparison between solution conductivity measured by a conductivity meter (open circles) and from the initial currents in the planar electrode cell (crosses).

( $B$ ) is determined from the slope of the data in Figures 4 and 5

$$I_0 = \frac{K}{B} V_0 \quad (8)$$

For the planar cell,  $B = \delta/A$  where  $A = 7.3$   $\text{cm}^2$  and  $\delta = 190$   $\mu$ m. In Figure 6 the values of  $K$  computed from the data and eq 8 are compared with the values measured using the conductivity meter. The agreement is quite good, reinforcing the conclusion that charge polarization at the electrodes had a negligible effect on the initial current.

The theoretical determination of  $B$  for the strip electrode cell is not straightforward as it is for the planar cell. Using a value for  $K$  measured independently with the conductivity meter, an experimental value of  $B$  is determined from eq 8. To determine  $B$  theoretically, we solve eq 7 for the electrical potential  $\Phi$ . The variables are nondimensionalized by using the width of each strip ( $w$ ) for the length scale and the potential of the center strip ( $V_0$ ) as the potential scale. The potential of the two outer



strip electrodes is held at ground ( $\Phi = 0$ ). The boundary conditions at time zero when the potential is first applied are

$$\begin{aligned} \text{on center electrode: } \Phi &= 1 \\ \text{on outer two electrodes: } \Phi &= 0 \\ \text{on glass surface: } \frac{\partial \Phi}{\partial y} &= 0 \end{aligned} \quad (9)$$

where  $x$  and  $y$  are the coordinates parallel and perpendicular to the bounding surfaces, respectively (see Figure 1b). These conditions assume negligible ohmic losses in the thin-film electrodes, which should be an excellent approximation given the low conductivity of the liquid. The boundary condition on the glass surfaces is a statement of zero current exchange between the liquid and the glass.

One more boundary condition is necessary to permit solution of eq 7. The fluid is unbounded laterally, so  $\Phi \rightarrow 0$  as  $x \rightarrow \pm\infty$ . To capture this condition we used the following boundary condition:

$$x = \pm\alpha: \frac{\partial \Phi}{\partial x} = 0 \quad (10)$$

where the coefficient  $\alpha$  is varied to see the effect on the numerical results. This boundary condition ensures there is no leakage of current outside the three strip electrodes.

We solved (7) with the above boundary conditions using FEMLAB, which generates two-dimensional meshes within the space. The gap  $h$  (i.e., the separation between the two slides) was varied from 0.5 to 10, and the center-to-center separation between the strips ( $b$ ) was set at 5, thereby matching the conditions of the experiment. We set  $\alpha = 3$ ; the results are insensitive to the value of  $\alpha$  above this value. The equations were solved in the half-plane  $x \geq 0$  using the additional symmetry condition

$$x = 0: \frac{\partial \Phi}{\partial x} = 0 \quad (11)$$

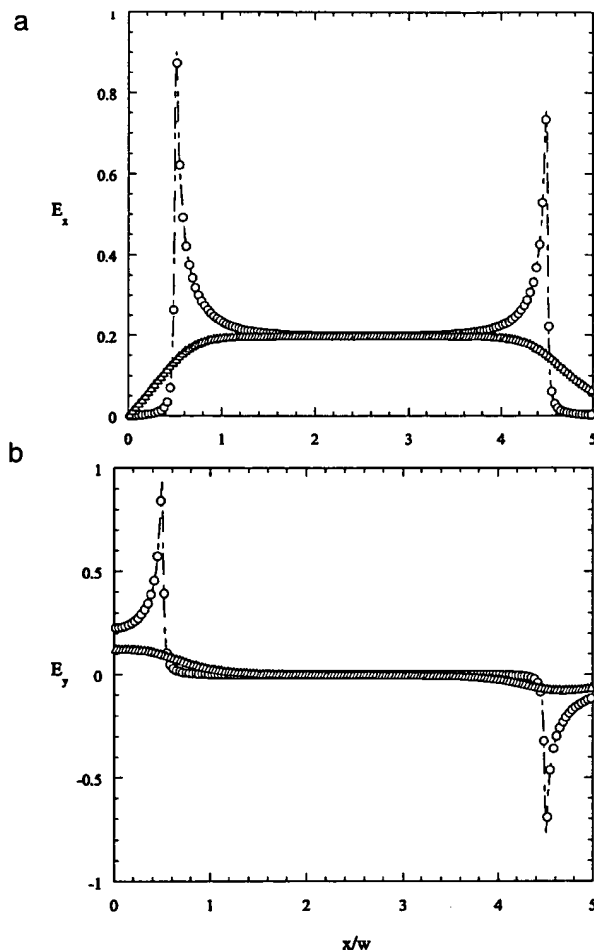
The mesh size was varied until the results converged.

Figure 7, panels a and b, shows the electric fields as a function of  $x$  for  $y = 0.0167$  (which equals the radius of a carbon black particle) and 0.5. As expected, the fields show large peaks at the edges of the electrodes; these fields are probably singular for an idealized step, but this behavior cannot be captured by the numerical solution. Note that  $E_x$  is essentially constant along the glass surface ( $y = 0.0167$ ) far from the edges of the strips, but increases by almost a factor of 5 near the edges.

The local current density within the liquid equals  $-K\nabla\Phi$ . The total current exchange between the center strip and the two outside strips is found by integrating the current density over the center strip electrode. Using the definition of  $B$  from eq 8, the theoretical value of the cell constant is

$$B = \frac{1}{2L \int_0^{L/2} \frac{\partial \Phi}{\partial y} dx} \quad (12)$$

where  $L$  is the length of the strips (2.4 cm). Figure 8 shows the effect of  $h$  on  $B$ . The two experimental values of  $B$  are also plotted in the figure. The good agreement between theory and experiment is further confirmation of a constant conductivity for these solutions over broad ranges of the electric field in the strip electrode cell.



**Figure 7.** Electric fields between strips as calculated from the theory. (a)  $E_x$  (b)  $E_y$ .  $h = 1$ . The fields are determined at  $y = 0.0166$  (open circle) and  $y = 0.5$  (open triangle)

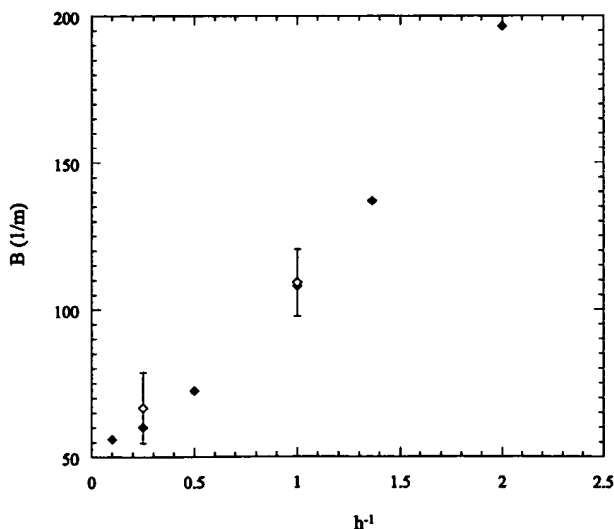


**Figure 8.** Cell constant ( $B$ ) of the strip electrode cell as a function of  $h$  (in units of  $w$ , see Figure 1). Filled diamond: theoretical calculation (eq 12,  $L = 2.4$  cm); open diamond: experimental result (eq 8).

**Short-Time Transients in the Currents.** The decay rate of the current in the limit  $t \rightarrow 0$  can be used along with the independently measured values of  $K$  to estimate

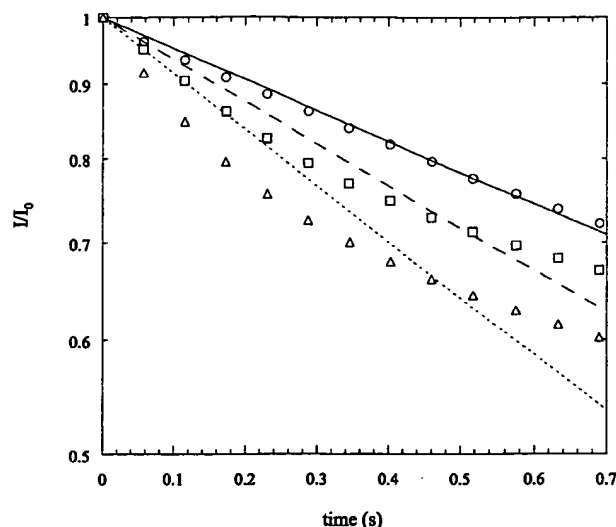


**Figure 9.** Current versus time in the planar electrode cell when  $V_0 = 1$  V. Circle: 0.50% OLOA; square: 1.57%; triangle: 3.63%. The lines are best fits of the data to eq 13.

both the concentration of pairs of charge carriers ( $C$ ) and the diffusion coefficient ( $D$ ) of each charge carrier. Here we use the data from the planar electrode cell because of the uniform current. We assume that the charge carrying species have equal mobilities and a valence of  $\pm 1$ .<sup>25</sup> Equation 2 is used to obtain the product  $DC$ , where the conductivity was determined from the initial current. The short-time decay of the current is assumed to be due to charge polarization at the electrodes. If we assume a constant capacity  $\hat{C}_E$  for each electrode and a constant resistance ( $R$ ) of the solution between the electrodes, we have the following expression for the current:

$$I = I_0 e^{-t/\tau} \quad (13)$$

where  $\tau = RC_E/2$ . Figure 9 shows a semilog plot of the current versus time for short times for three PIBS concentrations; the data do not follow eq 13. To obtain an estimate of  $\tau$  as  $t \rightarrow 0$ , we fit the data with an empirical expression of the form

$$I = I_0 e^{[-t/\tau + \beta t^2]} \quad (14)$$

The best fit of the data are shown as the curves in Figure 10. The values of  $\tau$  from these curves are listed in Table 1.

The current transient in nonpolar liquids is sometimes dependent on the applied potential. To check for any effects of applied potential, we measured the current transient as a function of  $V_0$ . The results are shown in Figure 11. The effect of  $V_0$  is small up to 5 V, but the data for 10 V are clearly different. The decay time constant  $\tau$  is independent of  $V_0$  for 5 V or less. Noting that  $I_0$  is proportional to  $V_0$  up to 10 V, it is possible that we would find  $\tau$  to be the same as for the lower potentials, but we did not take current readings at small enough times to allow an accurate determination of  $\tau$ .

The solution resistance is given by  $B/K$  with  $B = \delta/A$  for the planar electrodes. The capacitance of each electrode is assumed to equal the area of each electrode times the capacitance of the double layer per area ( $\hat{c}_{dl}$ ). Thus, the

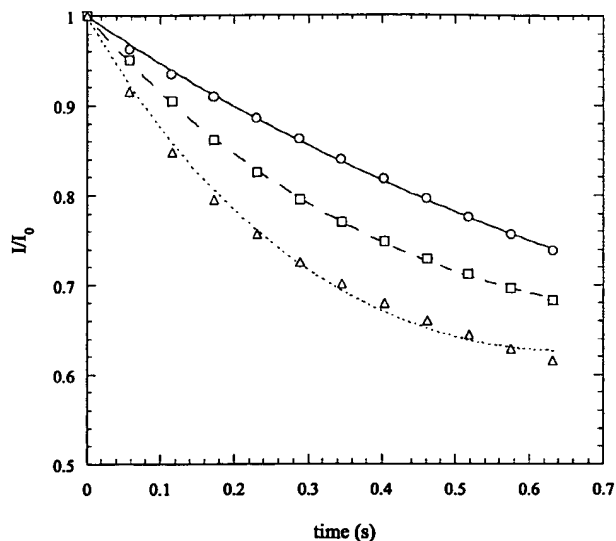


**Figure 10.** Same data as in Figure 9. The curves are best fits of the data to eq 14.

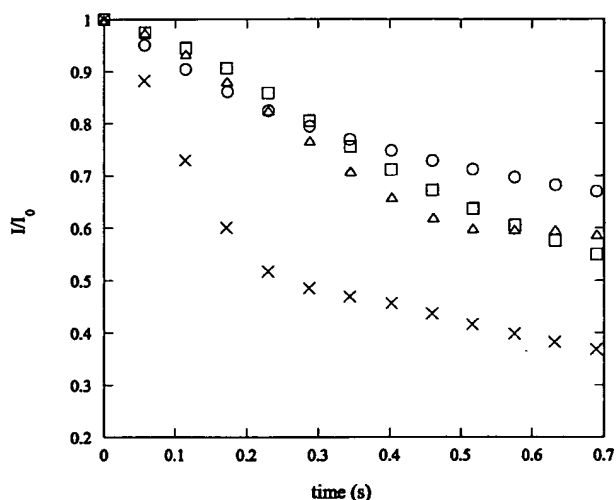


**Figure 11.** Current versus time in the planar electrode cell. 1.57% OLOA. circle:  $V_0 = 1$  V; square: 3 V; triangle: 5 V; cross: 10 V.

**Table 1. Solution Parameters Obtained from Experimental Determinations of  $K$  and  $\tau$ , and eq 21 for  $\alpha$ , eq 20 for  $C$ , eq 15 for  $\hat{c}_{dl}$ , and eq 16 for  $\kappa^{-1}$**

$C_{OL}$ (wt %)	$\tau$ (s)	$K$ (nS/m)	$\alpha$ (nm)	$C$ ( $\mu\text{mol}/\text{m}^3$ )	$\hat{c}_{dl}$ (mF/m <sup>2</sup> )	$\kappa^{-1}$ (nm)
0.50	1.77	2.86	9.4	21.3	53	332
1.57	1.04	8.98	10.3	73.2	99	179
3.63	0.68	20.8	10.0	164	148	120

double layer capacitance is related to the time constant of the initial current decay by

$$\tau = \frac{\delta \hat{c}_{dl}}{2K} \quad (15)$$

The values of  $\hat{c}_{dl}$  obtained from our experiments at the lowest applied potential are listed in Table 1. As discussed below,  $\hat{c}_{dl}$  is related to the concentration of charge carriers using the Gouy–Chapman theory of the double layer.

Assuming there is no mechanism to exchange charge between the ITO electrodes and the liquid phase, the charge in the double layer at each electrode builds up

with time because of the migration of the charge carriers toward or away from the electrode's surface. For traditional charge carrying species, for example simple ions in water, the thickness of the double layer is of order the Debye screening length of the solution

$$\kappa^{-1} = \left( \frac{\epsilon R_g T}{2z^2 F^2 C} \right)^{1/2} \quad (16)$$

Using the Gouy–Chapman model for the diffuse double layer, the differential capacitance per unit area is

$$\hat{c}_{dl} \equiv \frac{\partial \sigma}{\partial \Psi} = \left( \frac{2z^2 \epsilon F^2 C}{R_g T} \right)^{1/2} \cosh \left( \frac{\Psi}{2R_g T/zF} \right) \quad (17)$$

where  $z = 1$  here,  $\Psi$  is the potential drop over the double layer caused by the accumulation of charge,  $\epsilon$  is the dielectric permittivity of dodecane, and  $\sigma$  is the total net charge in the double layer per unit area. The minimum capacitance of the double layer occurs when  $\Psi = 0$

$$\hat{c}_{dl}^0 = \lim_{\Psi \rightarrow 0} \hat{c}_{dl} = \frac{\epsilon}{\kappa^{-1}} \quad (18)$$

According to the above model,  $|\Psi|$  must be less than  $2R_g T/F = 0.0514$  V for the capacitance to be approximately constant and equal to  $\hat{c}_{dl}^0$ . At  $V_0 = 1$  V this condition corresponds to a maximum of a 10% loss of the applied potential in the polarization layers at both electrodes; therefore, a linear relationship should only occur when  $I/I_0 > 0.9$  for this applied potential. This restriction on using (18) for the capacitance is the reason we determined  $\tau$  from the limiting slope of the data in Figure 10.

The two fundamental parameters of the solution are the concentration of pairs of charge carriers ( $C$ ) and the equivalent radius of the carriers ( $a$ ). The radius is determined from the diffusion coefficient using the Stokes–Einstein equation

$$a = \frac{R_g T}{6\pi\eta N_{avo} D} \quad (19)$$

where  $N_{avo}$  is the Avogadro number and  $\eta$  is the viscosity of the solution (0.0137 g/(cm s) for dodecane at 25 °C). By combining eqs 2 and 15–19, we obtain the following expressions for  $C$  and  $a$ :

$$C = \frac{2R_g T}{\epsilon F^2} \quad (20)$$

$$a = \frac{CF^2}{3\pi\eta N_{avo} K} \quad (21)$$

The values of  $C$  and  $a$  are listed in Table 1. The constancy of  $a$  as  $C_{OL}$  changes 7-fold is one validation of the model. Based on a similar approach but independent experiments with dodecane/OLOA-1200, Verschueren et al.<sup>25</sup> also determined 10 nm for the radius of the charge carrier. Kornbrenke<sup>15</sup> used a light scattering method to measure the equivalent radius of PIBS micelles (OLOA 1200 in dodecane) and obtained a value of about 5 nm. Morrison<sup>12</sup> cites data by Pugh et al.<sup>26</sup> that micelles of PIBS should have a radius of about 5 nm based on the length of the polymer chain. The fraction of PIBS molecules that form charged pairs ( $C/C_{OL}$ ) is listed in Table 2; the very small

**Table 2. Percentage of Micelles that Are Charged, Based Either on the Spherical ( $N_p$ ) or Spheroidal ( $N_m$ ) Geometry for the Micelles (Two Columns on the Right)<sup>a</sup>**

$C_{OL}$ (wt %)	$C_{OL}$ (mol/m <sup>3</sup> )	$C$ (μmol/m <sup>3</sup> )	$C/C_{OL}$ (10 <sup>-6</sup> )	$2CN_p/C_{OL}$ (%)	$2CN_m/C_{OL}$ (%)
0.50	2.20	21.3	9.68	2.5	1.6
1.57	7.04	73.2	10.4	2.7	1.7
3.63	16.6	164.1	9.88	2.6	1.6

<sup>a</sup>  $N_p = 1300$ ,  $N_m = 810$  PIBS molecules per micelle.

ratio (about 10 ppm) indicates that this system is a very weak electrolyte.

**Micelles as Charge Carriers.** The equivalent radius of the charge carriers (10 nm) indicates that they are aggregates of PIBS molecules, including impurities in the OLOA and probably water. Below we consider two geometric models for the micelles: a sphere with water assumed to fill the core and PIBS comprising the shell, and a prolate spheroid devoid of water whose diameter is twice the assumed length of a PIBS chain (5 nm). In these models, we assume the specific volume of both water and PIBS is 1 cm<sup>3</sup>/g.

If the micelles are spherical, then we expect the core to be water with  $N_w$  molecules, and the outer shell to be PIBS with  $N_p$  molecules. The core would be 5 nm in radius. A straightforward mass calculation, using 1700 for the molecular weight of PIBS, gives  $N_w = 17\,500$  and  $N_p = 1300$ . The fraction of micelles that are charged is given by  $2CN_p/C_{OL} = 2.6\%$  (see Table 2). The concentration of water required to fill the micelles, assuming all the PIBS is in the form of micelles, is 4.0 mg/cm<sup>3</sup> for the 3.63% OLOA solution. Demou et al.<sup>27</sup> found that pure dodecane can absorb water up to a concentration of 1 mg/cm<sup>3</sup> at 40% relative humidity. The water concentration is probably considerably higher in the present of OLOA. Thus, the core–shell spherical micelle model is plausible for our system. The moderately good reproducibility of our conductivity measurements in the absence of controlling water content is not inconsistent with this geometric model for the micelle because the micelle size is proportional to the cube root of the water content and hence is relatively insensitive to changes in the amount of water absorbed.

An alternative model which does not involve water is an elongated micelle, say a prolate spheroid of diameter  $d$  and length  $c$ . While the core would probably contain some water scavenged from the environment, we assume this water does not significantly contribute to the size of the micelle. The value of  $d$  is taken to be 10 nm, twice the length of PIBS molecules. The value of  $c$  must be determined from the Stokes–Einstein radius ( $a$ ) by equating the friction coefficient of a sphere ( $6\pi\eta a$ ) with that for the prolate spheroid

$$4\pi\eta ch(\gamma) = 6\pi\eta a, \quad h(\gamma) = \frac{3/4}{\ln(2/\gamma)} \quad (22)$$

where  $\gamma = d/c < 1$ . The above expression for  $h(\gamma)$  is an approximation based on slender body theory<sup>28,29</sup> and accounts for random orientations of the spheroid; because the error is of order  $\gamma^2 \ln \gamma$ , it is a good approximation for  $\gamma < 0.3$  and very accurate for  $\gamma < 0.1$ . Using  $a = 10$  nm and  $d = 10$  nm, the above equation yields  $\gamma = 0.23$  and hence  $c = 43.5$  nm. The aggregation number ( $N_m$  = number of PIBS molecules per micelle) is determined from the

(27) Demou, E.; Visram, H.; Donaldson, D. J.; Paul, P. A. *Atmos. Environ.* 2003, 37, 3529.

(28) Johnson, R. E. *J. Fluid Mech.* 1980, 99, 411.

(29) Solomentsev, Y.; Anderson, J. L. *J. Fluid Mech.* 1994, 279, 197.

(26) Pugh, R. J.; Matsunaga, T.; Fowkes, F. M. *Colloids Surf.* 1983, 7, 183.

volume of a micelle, and the specific volume ( $v_p$ ) and molecular weight ( $M_p$ ) of PIBS

$$N_m = \frac{\pi d^2 c N_{\text{avo}}}{6 v_p M_p} \quad (23)$$

where  $N_{\text{avo}}$  is Avogadro's number. Assuming  $v_p = 1 \text{ g/cm}^3$  (an estimate) and  $M_p = 1700$ , we have  $N_m = 810$ . Accepting this value of aggregation number, we then determine the fraction of micelles that carry a charge to be  $2CN_m/C_{\text{OL}} = 1.6\%$ .

The actual situation is probably between these two extreme geometric models. If this is the case, then we may conclude that the aggregation number of the micelles is between 810 and 1300.

**Electrode Charging and Nonlinear Equivalent Circuit.** The current in the planar electrode cell can be modeled using the Gouy–Chapman theory to relate  $\hat{c}_{\text{dl}}$  to the polarization potential  $\Psi$ . (This is not straightforward in the strip electrode cell because the current density varies spatially across each electrode.) The current density into the electrode is equal to  $KE$  where  $E$  is the electric field in the liquid outside the double layer. The rate of change of the charge density in the double layer ( $\sigma$ ) due to conduction in the liquid is given by

$$\frac{\partial \sigma}{\partial t} = \hat{c}_{\text{dl}}^0 \frac{\partial \Psi}{\partial t} = KE \quad (24)$$

Combining the above relations gives

$$\cosh\left(\frac{\Psi}{\Psi^*}\right) \frac{d\Psi}{dt} = \frac{KE}{\hat{c}_{\text{dl}}^0} \quad (25)$$

where  $\Psi^* = 2R_g T/F$ . The potential difference across the liquid gap ( $\Phi_0$ ) is less than the applied potential  $V_0$  because of the potential drop over the double layers of the two electrodes

$$\Phi_0 = V_0 - 2\Psi \quad (26)$$

The field in the bulk solution is given by  $E = \Phi_0/\delta$ . We define  $Y = \Phi(t)/V_0 = E(t)/E(0) = I(t)/I(0)$ ; the last equality holds as long as  $K$  is constant in the liquid. Integration of eq 25 gives the following for the nonlinear model of the current versus time

$$\int_Y^1 \cosh\left[\left(1 - \hat{Y}\right) \frac{V_0}{2\Psi^*}\right] \frac{d\hat{Y}}{\hat{Y}} = \left(\frac{2K}{\delta \hat{c}_{\text{dl}}^0}\right) t \quad (27)$$

The above must be numerically integrated to obtain  $Y$  ( $= I/I_0$ ) versus  $t$ . The linear model is recovered by setting  $V_0 = 0$

$$Y = \exp\left[-\left(\frac{2K}{\delta \hat{c}_{\text{dl}}^0}\right) t\right] \quad (28)$$

The current transients at  $V_0 = 3 \text{ V}$  for three different concentrations of PIBS are compared with the linear and nonlinear models in Figure 12. Remembering that there are no adjustable parameters, the linear model shows modest agreement with the data up to about 0.5 s. This is surprising because the double layer should be highly polarized given the amount of charge that is forced by the current toward or away from the electrode surface, thus increasing  $\Psi$  and the double layer capacitance. Note that if there were charge transfer across the solution/electrode interface, then the decay rate of the current should have

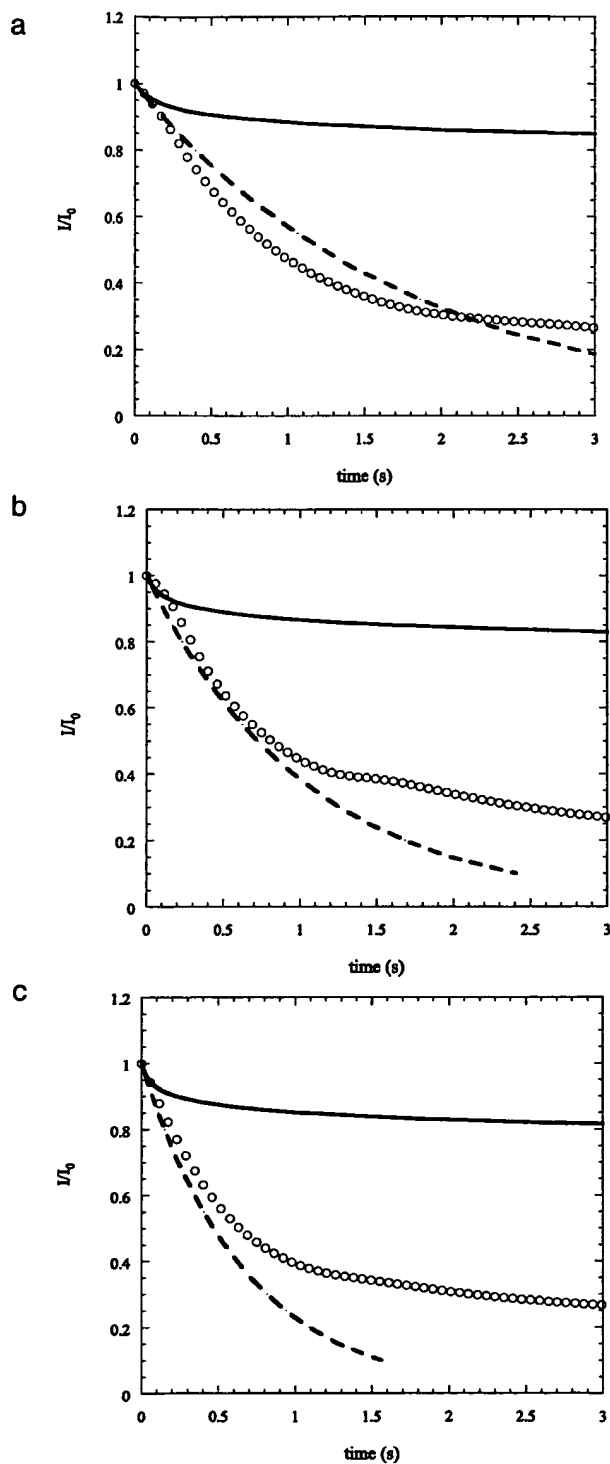


**Figure 12.** Experimental transient currents compared with theory based on perfectly polarized electrodes for the planar electrode cell.  $V_0 = 3 \text{ V}$ . (a) 0.50% OLOA/dodecane solution, (b) 1.57% OLOA, and (c) 3.63% OLOA. Circles: experimental data; solid line: nonlinear theory, eq 27; dashed line: linear theory, eq 28.

been less than the solid curves in Figure 12 (i.e., the data would lie above the solid curve). Below we consider why the model based on the Gouy–Chapman theory for the double layer (solid curve) fails to agree with the data.

Besides the low dielectric constant and weak nature of the electrolyte, a fundamental difference between our

system and solutions of simple electrolytes in water and other polar liquids is that the charge carriers (micelles) have a volume about  $10^5$  times that of a simple hydrated ion (radius  $\approx 0.2$  nm). This means that the volume fraction of charge carriers can quickly get to a limit where steric interactions among the carriers cause expansion of the double layer at the electrode surface. According to the classical Gouy–Chapman theory of the double layer, the total concentration of ionic charge carriers at the electrode surface would equal  $2C \cosh(2\Psi/\Psi^*)$ , so the local volume fraction represented by this charge density would be

$$\phi_s = 2v_m N_a C \cosh\left(\frac{2\Psi}{\Psi^*}\right) \quad (29)$$

where  $N_a$  is Avogadro's number and  $v_m$  is the volume of one ionic charge carrier (here,  $4190 \text{ nm}^3$  using the sphere model for the micelle). For example, consider  $C = 164 \text{ } \mu\text{moles/m}^3$ , which corresponds to the condition for the data shown in Figure 12c. At a polarization potential of  $\Psi = 100 \text{ mV}$  at each electrode, the volume fraction of micelles at the electrode surface is already predicted to be 2%, which violates the primary assumption of the Gouy–Chapman theory, namely the existence of point ions. Clearly the Gouy–Chapman theory breaks down at modest polarization potentials with these macroions.

Another estimate of the steric crowding of charge carriers in the double layer is made by considering the charge transferred in the cell and assuming no charge transfer across the electrode surface. The total charge transferred over time  $t$  is given by

$$Q(t) = \int_0^t I \, dt \quad (30)$$

The integral over the first three seconds gives  $0.06$ ,  $0.16$ , and  $0.31 \text{ } \mu\text{C}$  for the data plotted in Figure 12a–c, respectively. The area ( $A$ ) of each electrode is  $7.3 \text{ cm}^2$ . Dividing these values by  $2A\kappa^{-1}$ , where  $\kappa^{-1}$  is computed from (16), we obtain an estimate of the mean volume fraction of ions in the double layer

$$\phi = \frac{N_a Q v_m}{2A\kappa^{-1}F} \quad (31)$$

Using  $4190 \text{ nm}^3$  for the micelle volume  $v_m$ , we estimate a mean volume fraction of the charge carriers in the double layer to be 4.7% after three seconds for the data plotted in Figure 12c.

The steric crowding of charged micelles in the double layer would expand the diffuse region, and the double layer thickness ( $\lambda$ ) would exceed the value of the Debye screening length. Because  $\epsilon_{dl}^0 \sim \lambda^{-1}$ , the capacitance of the double layers would not increase as rapidly with  $\Psi$  as expected from the Gouy–Chapman model; therefore,  $\Psi$  would increase faster than predicted, resulting in a current decaying faster than predicted by eq 27. While the Gouy–Chapman theory has been modified to allow for finite ion size,<sup>30–34</sup> none of these modifications considers volume fractions of ions as high as 1%.

Another possible explanation for the disagreement between experimental results and theory is the math-

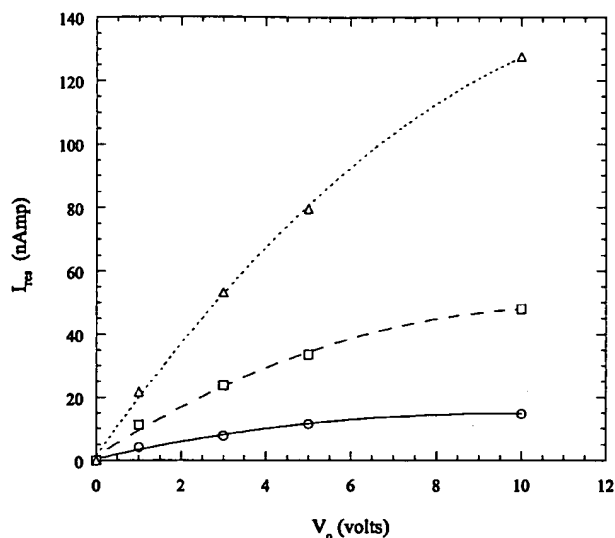


**Figure 13.** Residual currents in the planar electrode cell measured 10 s after application of the potential  $V_0$ . Circle: 0.50% OLOA; square: 1.57% OLOA; triangle: 3.63% OLOA. The curves are 2nd order polynomial best fits to the data.

ematical approximation made in the theory itself. In our theory, we have divided the liquid gap into two regions: (1) the double layer near the electrode surface, for which the classical Gouy–Chapman theory is used and (2) the “bulk” region where electroneutrality is assumed and eq 7 holds. For this approximation to be valid, the thickness of the double layer must be negligible compared to the gap distance, and depletion of the charge carriers in the bulk solution must be negligible. Even if the polarized double layer is 10 times greater than the initial Debye length ( $\approx 200 \text{ nm}$ ), its thickness is still 2 orders of magnitude smaller than the gap  $\delta$  in the planar cell. The question of depleting charge carriers is answered by considering the total charge ( $0.31 \text{ } \mu\text{C}$ ) carried from the solution after 3 s for the 3.63% OLOA solution. Comparing this charge with the total charge ( $4.4 \text{ } \mu\text{C}$ ) existing at time zero in the solution indicates that the depletion of charge carriers was at most 7% over this time, even assuming no new charge carriers were produced through the mechanism depicted in eq 1.

**Residual Currents.** After about 10 s, the current remained at a nearly constant value for long times, with only a slow decrease with time over minutes up to hours. We observed these long-time currents in both electrode configurations, and the value was typically 5–10% of the initial current. We define the “residual current”  $I_{res}$  as the current at 10 s after application of the potential. Figure 13 shows the value of  $I_{res}$  versus applied potential for the three OLOA concentrations. These currents are not proportional  $V_0$ ; however, they are roughly proportional to  $C_{OL}$  at fixed  $V_0$ .

One issue related to residual currents is possible depletion of charge carriers in the solution. Since the equilibrium of eq 1 is far to the left, the reservoir of potential charge carriers is the uncharged micelles. As charge carriers are forced to the electrodes, more charge carriers are formed in the solution. Thus, the maximum potential charge is proportional to the micelle concentration

$$Q_{max} = \frac{C_{OL} F V_c}{N_p} \quad (32)$$

(30) Outhwaite, C. W. *Chem Phys Lett* 1980, 76, 619.

(31) Carnie, S. L.; Chan, D. Y. C. *J. Chem. Phys.* 1980, 73, 2949.

(32) Snook, I.; van Megen, W. *J. Chem. Phys.* 1981, 75, 4104.

(33) Torrie, G. M.; Kuslik, P. G.; Patey, G. N. *J. Chem. Phys.* 1989, 91, 6367.

(34) Bohinc, K.; Kralj-Iglic, V.; Iglic, A. *Electrochim. Acta* 2001, 46, 3033.

where  $V_c$  is the volume of the solution in the cell. For 3.6% OLOA concentration in the planar cell (see Table 2 for  $C_{OL}$ ),  $Q_{max} = 170 \mu\text{C}$ . From Figure 13, we have  $I_{res} = 80 \text{ nA}$  for  $V_0 = 5 \text{ V}$ . Even if this value continued for only 1 h,  $Q = 280 \mu\text{C}$  of charge is transferred through the cell, which is the capacity of the micellar solution. Yet we observed the residual current to last as long as 8 h in one experiment at a lower potential. Thus, although much of the long-term current can be ascribed to normal conductive processes and electrode polarization, there was an insufficient reservoir of charge carriers to continue the current over the very long times as was observed. Furthermore, as the micelle concentration was depleted in the bulk solution, the conductivity should have been proportionally reduced, thus decreasing the current much faster than we observed. We conclude that some charge transfer across the solution/ITO interface must have occurred over long times.

### Conclusions

Our experimental results show that OLOA/dodecane solutions behave as conventional electrolyte solutions for short times after application of the potential difference. The linear current/potential relationship was observed over the range 5–500 kV/m electric fields in both one-dimensional or two-dimensional fields. The solution conductivity is proportional to the concentration of OLOA, as observed by others. To our knowledge an ohmic response has not previously been demonstrated with such complex nonpolar fluid/charge control agent solutions in two-dimensional fields. Our determination of the electrical cell constant for the strip electrode configuration using a numerical solution to Laplace's equation matches the experimentally derived value at two cell thicknesses. These results taken as a whole demonstrate that eq 7 applies to OLOA/dodecane solutions when electrode polarization is minimal.

Perhaps the most important result of this work is the determination of the size of the charge carriers in this system. The analysis of the short-time current decay using the classical theory of the double layer at the electrode surface leads to an equivalent micelle radius of 10 nm for all three concentrations of OLOA. The fact that the

dynamics of the current gives the same radius across a 7-fold change in OLOA concentration is significant support for the model envisioning the charge carriers are micelles in the classical sense, that is, the micelle size is independent of surfactant concentration. The experimental radius of 10 nm can be reconciled with the size of the PIBS molecule (5 nm) by assuming a spherical micelle with water in the core or a nonspherical shape made up only of PIBS molecules. The aggregation number is 1300 PIBS molecules per micelle for the first model and 810 for the second (assuming a prolate spheroid).

The current at intermediate times (0.5–3 s) decays faster than predicted by modeling the capacitance of the polarized double layers on the electrode surfaces using the Gouy–Chapman theory. We suggest that some of the discrepancy between data and theory is due to an expansion of the diffuse region of the double layer because of steric crowding of the charge carriers. The volume of the charge carriers here is of order  $10^5$  times that for simple ions in polar liquids such as water. Steric crowding would lead to diffuse regions thicker than the conventionally defined Debye screening length, thus reducing the capacitance of the double layer as the charge builds up. Another possible source of discrepancy is the mathematical approximation we made in the theory by dividing the liquid gap into a double layer and a bulk region, and assuming the electric field and concentration gradients of the charge carriers in the latter are negligible compared to their values in the double layer.

Further work on solutions such as OLOA/dodecane is needed in three areas. First, analytical methods such as light scattering are needed to determine both the size and shape of the micelles. Second, the kinetics of charge creation, related to the mass action law given in (1) and the rate term  $r_i$  in (5), needs to be examined. This could possibly be done with *ac* potentials over a range of frequency. The ability of the micelles to create and destroy charge through collisions adds a new dimension to modeling the charge transport in these fluids. Finally, the structure of the double layer with these large ions needs more attention.

LA040110+